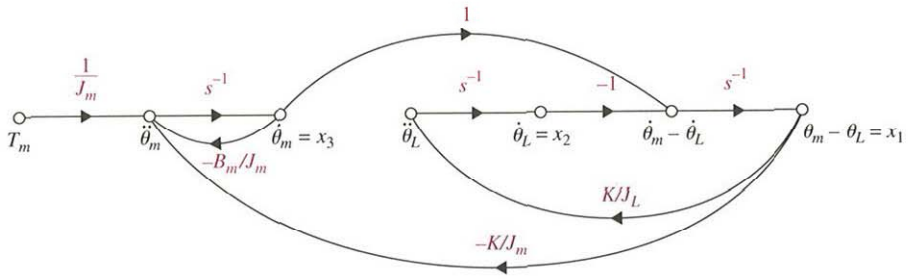

Figure 4-25 State diagram of the system of Fig. 4-24.

The transfer functions between $\Theta_m(s)$ and $T_m(s)$ and $\Theta_L(s)$ and $T_m(s)$ are written by applying the gain formula to the state diagram in Fig. 4-25:

$$\frac{\Theta_m(s)}{T_m(s)} = \frac{X_3(s)}{sT_m(s)} = \frac{J_L s^2 + K}{s[J_m J_L s^3 + B_m J_L s^2 + K(J_m + J_L)s + B_m K]} \tag{4-88}$$

$$\frac{\Theta_L(s)}{T_m(s)} = \frac{X_2(s)}{sT_m(s)} = \frac{K}{s[J_m J_L s^3 + B_m J_L s^2 + K(J_m + J_L)s + B_m K]} \tag{4-89}$$

▲

4-5 Sensors and Encoders in Control Systems

Sensors and encoders are important components used to monitor the performance and for feedback in control systems. In this section the principle of operation and applications of some of the sensors and encoders that are commonly used in control systems are described.

4-5-1 Potentiometer

A potentiometer is an electromechanical transducer that converts mechanical energy into electrical energy. The input to the device is in the form of a mechanical displacement, either linear or rotational. When a voltage is applied across the fixed terminals of the potentiometer, the output voltage, which is measured across the variable terminal and ground, is proportional to the input displacement, either linearly or according to some nonlinear relation.

Rotary potentiometers are available commercially in single-revolution or multirevolution form, with limited or unlimited rotational motion. The potentiometers commonly are made with wirewound or conductive plastic resistance material. Figure 4-26 shows a rotary potentiometer, and Fig. 4-27 shows linear potentiometer that contains a built-in operational amplifier. For precision control, the conductive plastic potentiometer is preferable, since it has infinite resolution, long rotational life, good output smoothness, and low static noise.

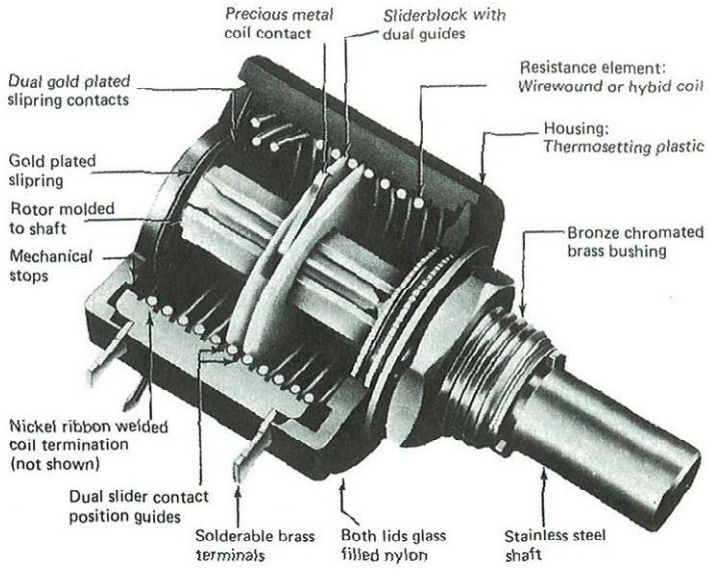

Figure 4-26 *Ten-turn rotary potentiometer.* (*Courtesy of* Helipot Divison of Beckman Instruments, Inc.)

Figure 4-28 shows the equivalent-circuit representation of a potentiometer, linear or rotary. Since the voltage across the variable terminal and reference is proportional to the shaft displacement of the potentiometer, when a voltage is applied across the fixed terminals, the device can be used to indicate the absolute position of a system or the relative position of two mechanical outputs. Figure 4-29(a) shows the arrangement

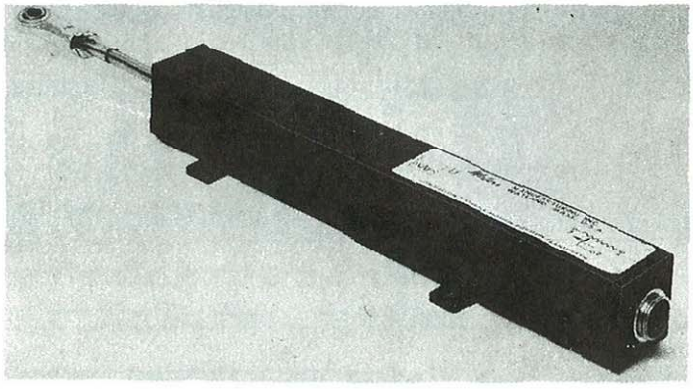

Figure 4-27 *Linear motion potentiometer with built-in operational amplifier.* (Courtesy of Waters Manufacturing, Inc.)

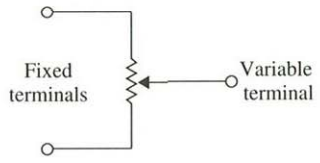

Figure 4-28 Circuit representation of a potentiometer.

when the housing of the potentiometer is fixed at reference; the output voltage $e(t)$ will be proportional to the shaft position $\theta_c(t)$ in the case of a rotary motion. Then

$$e(t) = K_s \theta_c(t) \tag{4-90}$$

where K_s is the proportional constant. For an N-turn potentiometer, the total displacement of the variable arm is $2\pi N$ radians. The proportional constant K_s is given by

$$K_s = \frac{E}{2\pi N} \quad \text{V/rad} \tag{4-91}$$

where E is the magnitude of the reference voltage applied to the fixed terminals. A more flexible arrangement is obtained by using two potentiometers connected in parallel, as shown in Fig. 4-29(b). This arrangement allows the comparison of two remotely located shaft positions. The output voltage is taken across the variable terminals of the two potentiometers and is given by

$$e(t) = K_s[\theta_1(t) - \theta_2(t)] \tag{4-92}$$

Figure 4-30 illustrates the block diagram representation of the setups in Fig. 4-29.

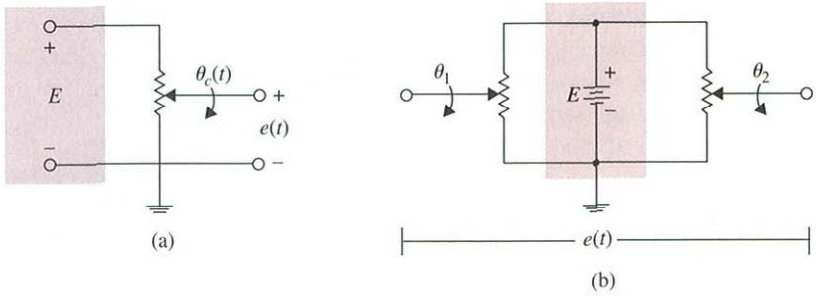

Figure 4-29 (a) Potentiometer used as a position indicator. (b) Two potentiometers used to sense the positions of two shafts.

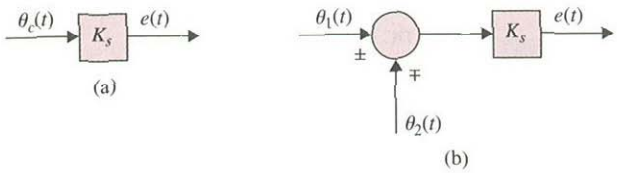

Figure 4-30 Block diagram representations of potentiometer arrangements in Fig. 4-29.

In dc-motor control systems, potentiometers are often used for position feedback. Figure 4-31(a) shows the schematic diagram of a typical dc-motor position-control system. The potentiometers are used in the feedback path to compare the actual load position with the desired reference position. If there is a discrepancy between the load position and the reference input, an error signal is generated by the potentiometers that will drive the motor in such a way that this error is minimized quickly. As shown in Fig. 4-31(a), the error signal is amplified by a dc amplifier whose output drives the armature of a permanent-magnet dc motor. Typical waveforms of the signals in the system when the input $\theta_r(t)$ is a step function are shown in Fig. 4-31(b). Note that the electric signals are all unmodulated. *In control systems terminology, a dc signal usually refers to an unmodulated signal. On the other hand, an ac signal refers to signals that are modulated by a modulation process.* These definitions are different from those commonly used in electrical engineering, where dc refers simply to unidirectional signals and ac indicates alternating signals.

▲ In control-system terminology, a dc signal usually refers to an unmodulated signal.

Figure 4-32(a) illustrates a control system that serves essentially the same purpose as that of the system in Fig. 4-31(a), except that ac signals prevail. In this case the voltage applied to the error detector is sinusoidal. The frequency of this signal is usually much higher than that of the signal that is being transmitted through the system. Control systems with ac signals are usually found in aerospace systems that are more susceptible to noise.

Typical signals of the ac control system are shown in Fig. 4-32(b). The signal $v(t)$ is referred to as the carrier whose frequency is ω_c, or

$$v(t) = E \sin \omega_c t \tag{4-93}$$

Analytically, the output of the error signal is given by

$$e(t) = K_s \theta_e(t) v(t) \tag{4-94}$$

where $\theta_e(t)$ is the difference between the input displacement and the load displacement, or

$$\theta_e(t) = \theta_r(t) - \theta_r(t) \tag{4-95}$$

For the $\theta_e(t)$ shown in Fig. 4-32(b), $e(t)$ becomes a **suppressed-carrier-modulated** signal. A reversal in phase of $e(t)$ occurs whenever the signal crosses the zero-magnitude axis. This reversal in phase causes the ac motor to reverse in direction according to the desired sense of correction of the error signal $\theta_e(t)$. The name *suppressed-carrier*

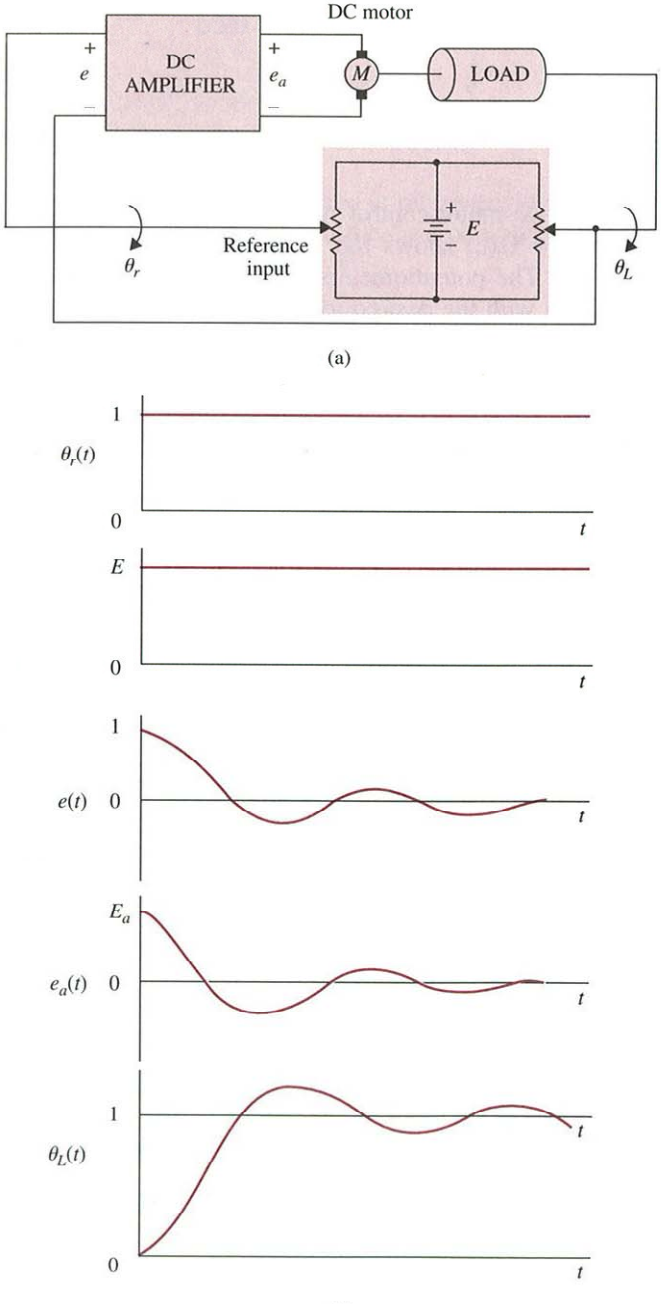

Figure 4-31 (a) Dc-motor position-control system with potentiometers as error sensors. (b) Typical waveforms of signals in the control system of part (a).

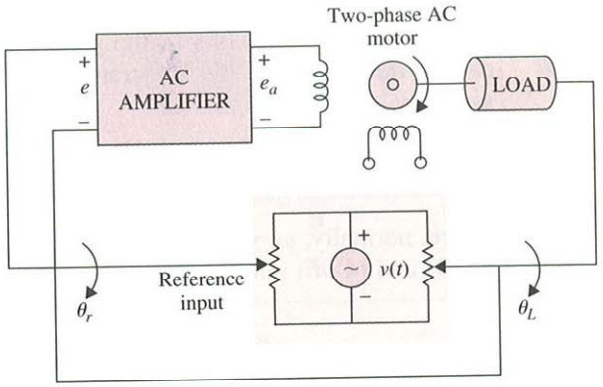

(a)

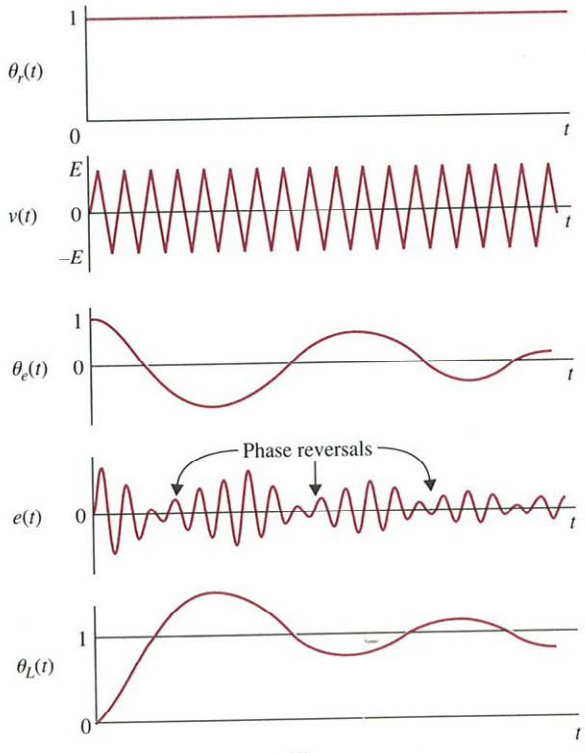

(b)

Figure 4-32 (a) Ac control system with potentiometers as error detectors. (b) Typical waveforms of signals in the control system of part (a).

modulation stems from the fact that when a signal $\theta_e(t)$ is modulated by a carrier signal $v(t)$ according to Eq. (4-94), the resultant signal $e(t)$ no longer contains the original carrier frequency ω_c. To illustrate this, let us assume that $\theta_e(t)$ is also a sinusoid given by

$$\theta_e(t) = \sin \omega_s t \tag{4-96}$$

where, normally, $\omega_s \ll \omega_c$. By use of familiar trigonometric relations, substituting Eqs. (4-93) and (4-96) into Eq. (4-94), we get

$$e(t) = \tfrac{1}{2}K_s E[\cos(\omega_c - \omega_s)t - \cos(\omega_c + \omega_s)t] \tag{4-97}$$

Therefore, $e(t)$ no longer contains the carrier frequency ω_c or the signal frequency ω_s, but has only the two sidebands $\omega_c + \omega_s$ and $\omega_c - \omega_s$.

When the modulated signal is transmitted through the system, the motor acts as a demodulator, so that the displacement of the load will be of the same form as the dc signal before modulation. This is seen clearly from the waveforms of Fig. 4-32(b). It should be pointed out that a control system need not contain all-dc or all-ac components. It is quite common to couple dc component to an ac component through a modulator or an ac device to a dc device through a demodulator. For instance, the dc amplifier of the system in Fig. 4-31(a) may be replaced by an ac amplifier that is preceded by a modulator and followed by a demodulator.

4-5-2 Tachometers

Tachometers are electromechanical devices that convert mechanical energy into electrical energy. The device works essentially as a voltage generator, with the output voltage proportional to the magnitude of the angular velocity of the input shaft. In control systems, most of the tachometers used are of the dc variety (i.e., the output voltage is

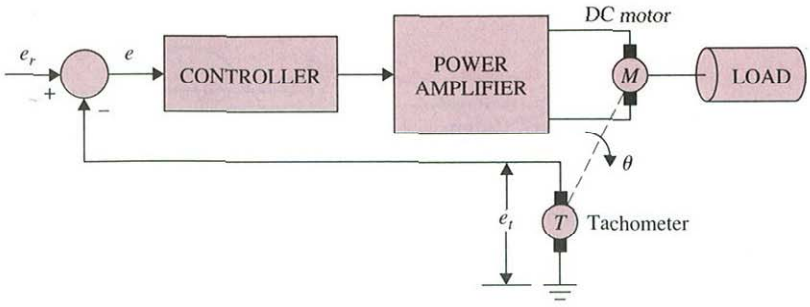

Figure 4-33 Velocity-control system with tachometer feedback.

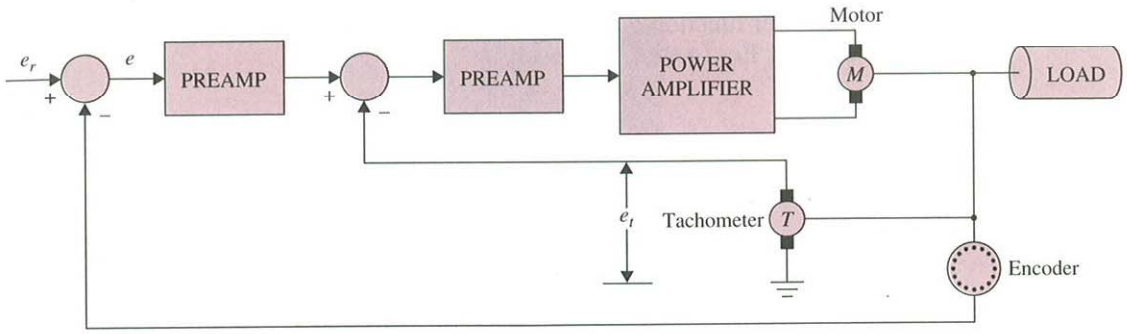

Figure 4-34 Position-control system with tachometer feedback.

a dc signal). Dc tachometers are used in control systems in many ways; they can be used as velocity indicators to provide shaft-speed readout or to provide velocity feedback or speed control or stabilization. Figure 4-33 is a block diagram of a typical velocity-control system in which the tachometer output is compared with the reference voltage, which represents the desired velocity to be achieved. The difference between the two signals, or the error, is amplified and used to drive the motor, so that the velocity will eventually reach the desired value. In this type of application, the accuracy of the tachometer is highly critical, as the accuracy of the speed control depends on it.

▲ *Note:* Tachometers are often used in control systems to improve stability.

In a position-control system, velocity feedback is often used to improve the stability or the damping of the closed-loop system. Figure 4-34 shows the block diagram of such an application. In this case the tachometer feedback forms an inner loop to improve the damping characteristics of the system, and the accuracy of the tachometer is not so critical.

The third and most traditional use of a dc tachometer is in providing the visual speed readout of a rotating shaft. Tachometers used in this capacity are generally connected directly to a voltmeter calibrated in revolutions per minute (rpm).

Mathematical Modeling of Tachometers

The dynamics of the tachometer can be represented by the equation

$$e_t(t) = K_t \frac{d\theta(t)}{dt} = K_t\omega(t) \tag{4-98}$$

where $e_t(t)$ is the output voltage, $\theta(t)$ the rotor displacement in radians, $\omega(t)$ the rotor velocity in rad/sec, and K_t the **tachometer constant** in V/rad/sec. The value of K_t is usually given as a catalog parameter in **volts per 1000 rpm** (V/krpm).

The transfer function of a tachometer is obtained by taking the Laplace transform on both sides of Eq. (4-98). The result is

$$\frac{E_t(s)}{\Theta(s)} = K_t s \tag{4-99}$$

where $E_t(s)$ and $\Theta(s)$ are the Laplace transforms of $e_t(t)$ and θ(t), respectively.

4-5-3 Incremental Encoder

Incremental encoders are frequently found in modern control systems for converting linear or rotary displacement into digitally coded or pulse signals. The encoders that output a digital signal are known as **absolute encoders.** In the simplest terms, absolute encoders provide as output a distinct digital code indicative of each particular least significant increment of resolution. **Incremental encoders,** on the other hand, provide a pulse for each increment of resolution but do not make distinctions between the increments. In practice, the choice of which type of encoder to use depends on economics and control objectives. For the most part, the need for absolute encoders has much to do with the concern for data loss during power failure or the applications involving periods of mechanical motion without the readout under power. However, the incremental encoder's simplicity in construction, low cost, ease of application, and versatility have made it by far one of the most popular encoders in control systems.

Incremental encoders are available in rotary and linear forms. Figures 4-35 and 4-36 show typical rotary and linear incremental encoders, respectively. A typical rotary incremental encoder has four basic parts: a light source, a rotary disk, a stationary mask, and a sensor, as shown in Fig. 4-37. The disk has alternate opaque and transparent sectors. Any pair of these sectors represents an incremental period. The mask is used to pass or block the light beam between the light source and the photosensor located behind the mask. For encoders with relatively low resolution, the mask is not necessary. For fine-resolution encoders (up to thousands of increments per revolution), a multiple-slit mask is often used to maximize reception of the shutter light.

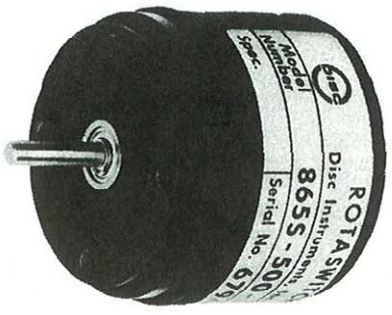

Figure 4-35 Rotary incremental encoder. (Courtesy of DISC Instruments, Inc.)

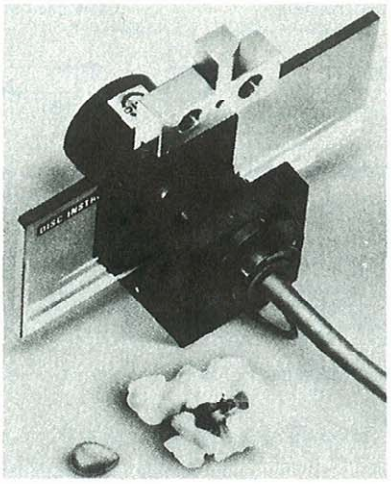

Figure 4-36 Linear incremental encoder. (Courtesy of DISC Instruments, Inc.)

The waveforms of the sensor outputs are generally triangular or sinusoidal, depending on the resolution required. Square-wave signals compatible with digital logic are derived by using a linear amplifier followed by a comparator. Figure 4-38(a) shows a typical rectangular output waveform of a single-channel incremental encoder. In this case pulses are produced for both directions of shaft rotation. A dual-channel encoder with two sets of output pulses is necessary for direction sensing and other control functions. When the phase of the two-output pulse train is 90° apart electrically, the two signals are said to be in quadrature, as shown in Fig. 4-38(b); the signals uniquely define 0-to-1 and 1-to-0 logic transitions with respect to the direction of rotation of the encoder disk, so that a direction-sending logic circuit can be constructed to decode the signals. Figure 4-39 shows the single-channel output and the quadrature outputs with sinusoidal waveforms. The sinusoidal signals from the incremental encoder can be used for fine-position control in feedback control systems. The following example illustrates some applications of the incremental encoder in control systems.

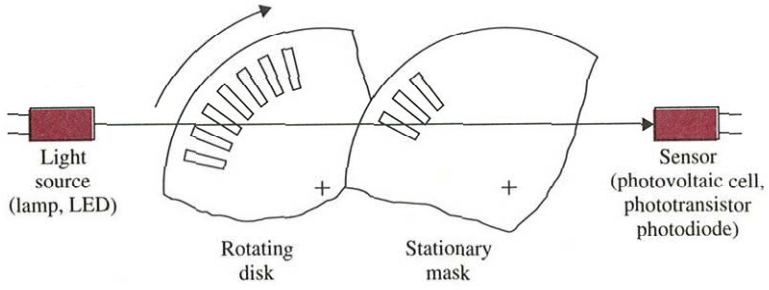

Figure 4-37 Typical increment optomechanics.

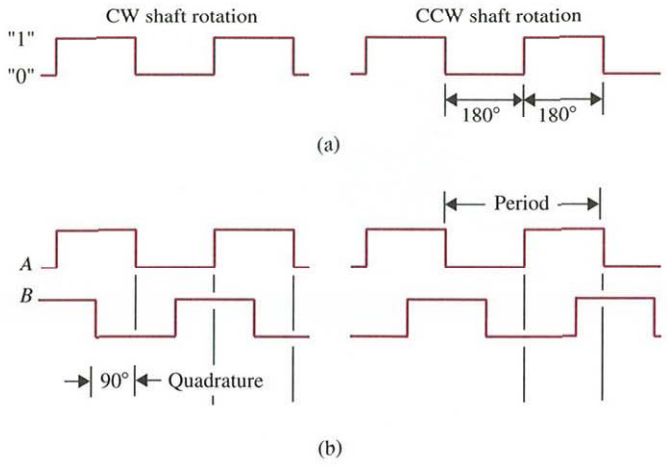

Figure 4-38 (a) Typical rectangular output waveform of a single-channel encoder device (bidirectional). (b) Typical dual-channel encoder signals in quadrature (bidirectional).

Example 4-9

Consider an incremental encoder that generates two sinusoidal signals in quadrature as the encoder disk rotates. The output signals of the two channels are shown in Fig. 4-40 over one cycle. Note that the two encoder signals generate four zero crossings per cycle. These zero crossings can be used for position indication, position control, or speed measurements in control systems. Let us assume that the encoder shaft is coupled directly to the rotor shaft of a motor that directly drives the printwheel of an electronic typewriter or word processor. The printwheel has 96 character positions on its periphery, and the encoder has 480 cycles. Thus there are $480 \times 4 = 1920$ zero crossings per revolution. For the 96-character printwheel, this corresponds

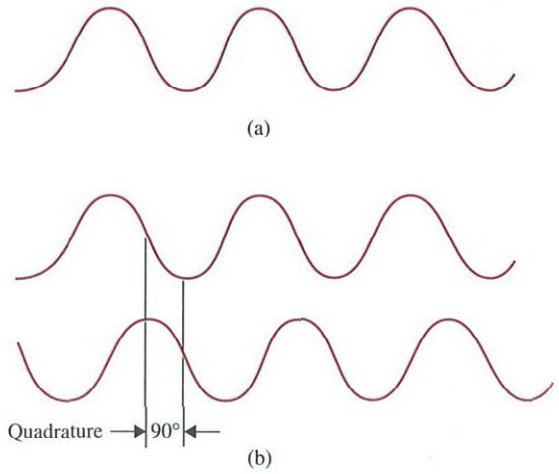

Figure 4-39 (a) Typical sinusoidal output waveform of a single-channel encoder device. (b) Typical dual-channel encoder signals in quadrature.

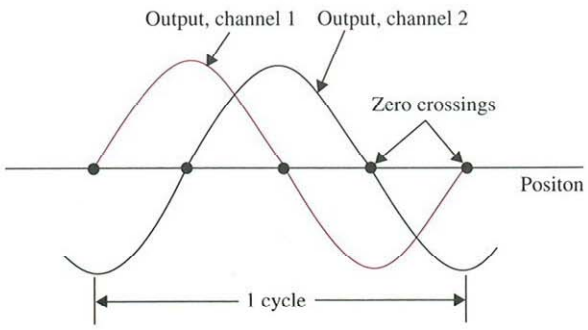

Figure 4-40 One cycle of the output signals of a dual-channel incremental encoder.

to 1920/96 = 20 zero crossings per character; that is, there are 20 zero crossings between two adjacent characters.

One way of measuring the velocity of the printwheel is to count the number of pulses generated by an electronic clock that occur between consecutive zero crossings of the encoder outputs. Let us assume that a 500-kHz clock is used (i.e., the clock generates 500,000 pulses/sec). If the counter counts, say 500 clock pulses while the encoder rotates from the zero crossing to the next, the shaft speed is

$$\begin{aligned}\frac{500{,}000 \text{ pulses/sec}}{500 \text{ pulses/zero crossing}} &= 1000 \text{ zero crossings/sec} \\ &= \frac{1000 \text{ zero crossings/sec}}{1920 \text{ zero crossings/sec}} = 0.52083 \text{ rev/sec} \\ &= 31.25 \text{ rpm}\end{aligned} \tag{4-100}$$

The encoder arrangement described can be used for fine-position control of the printwheel. Let the zero crossing A of the waveforms in Fig. 4-40 correspond to a character position on the printwheel (the next character position is 20 zero crossings away), and the point corresponds to a stable equilibrium point. The coarse-position control of the system must first drive the printwheel position to within one zero crossing on either side of position A; then by using the slope of the sine wave at position A, the control system should null the error quickly. ▲

4-6 DC Motors in Control Systems

Direct-current (dc) motors are one of the most widely used prime movers in industry today. Years ago a majority of the small servomotors used for control purposes were of the ac variety. In reality, ac motors are more difficult to control, especially for position control, and their characteristics are quite nonlinear, which makes the analytical task more difficult. Dc motors, on the other hand, are more expensive, because of the brushes and commutators, and variable-flux dc motors are suitable only for certain types of control applications. Before permanent-magnet technology was fully developed, the

torque per unit volume or weight of a dc motor with a permanent-magnet (PM) field was far from desirable. Today, with the development of the rare-earth magnet, it is possible to achieve very high torque-to-volume PM dc motors at reasonable cost. Furthermore, the advances made in brush-and-commutator technology have made these wearable parts practically maintenance-free. The advancements made in power electronics have made brushless dc motors quite popular in high-performance control systems. Advanced manufacturing techniques have also produced dc motors with ironless rotors that have very low inertia, thus achieving a very high torque-to-inertia ratio, and low-time-constant properties have opened new applications for dc motors in computer peripheral equipment such as tape drives, printers, disk drives, and word processors, as well as in the automation and machine-tool industries.

4-6-1 Basic Operational Principles of DC Motors

The dc motor is basically a torque transducer that converts electric energy into mechanical energy. The torque developed on the motor shaft is directly proportional to the field flux and the armature current. As shown in Fig. 4-41, a current-carrying conductor is established in a magnetic field with flux ϕ, and the conductor is located at a distance r from the center of rotation. The relationship among the developed torque, flux ϕ, and current i_a is

$$T_m = K_m \phi i_a \tag{4-101}$$

where T_m is the motor torque (N-m, lb-ft, or oz-in.), ϕ the magnetic flux (webers), i_a the armature current (amperes), and K_m is a proportional constant.

In addition to the torque developed by the arrangement shown in Fig. 4-41, when the conductor moves in the magnetic field, a voltage is generated across its terminals. This voltage, the **back emf,** which is proportional to the shaft velocity, tends to oppose the current flow. The relationship between the back emf and the shaft velocity is

$$e_b = K_m \phi \omega_m \tag{4-102}$$

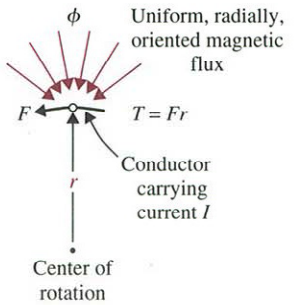

Figure 4-41 Torque production in a dc motor.

where e_b denotes the back emf (volts), and ω_m is the shaft velocity (rad/sec) of the motor. Equations (4-101) and (4-102) form the basis of the dc-motor operation.

4-6-2 Basic Classifications of PM DC Motors

In general, the magnetic field of a dc motor can be produced by field windings or permanent magnets. Due to the popularity of PM dc motors in control system applications, we concentrate on this type of motor. PM dc motors can be classified according to commutation scheme and armature design. Conventional dc motors have mechanical brushes and commutators. However, in one important class of dc motors the commutation is done electronically; this type of motor is called a **brushless dc motor.**

According to the armature construction, the PM dc motor can be broken down into three types of armature design: **iron-core, surface-wound,** and **moving-coil** motors.

Iron-Core PM DC Motors

The rotor and stator configuration of an iron-core PM dc motor is shown in Fig. 4-42. The permanent-magnet material can be barium–ferrite, Alnico, or rare-earth compound. The magnetic flux produced by the magnet passes through a liminated rotor structure that contains slots. The armature conductors are placed in the rotor slots. This type of dc motor is characterized by relatively high rotor inertia (since the rotating part consists of the armature windings), high inductance, low cost, and high reliability.

Surface-Wound DC Motors

Figure 4-43 shows the rotor construction of a surface-wound PM dc motor. The armature conductors are bonded to the surface of a cylindrical rotor structure, which is made of laminated disks fastened to the motor shaft. Since no slots are used on the rotor in this

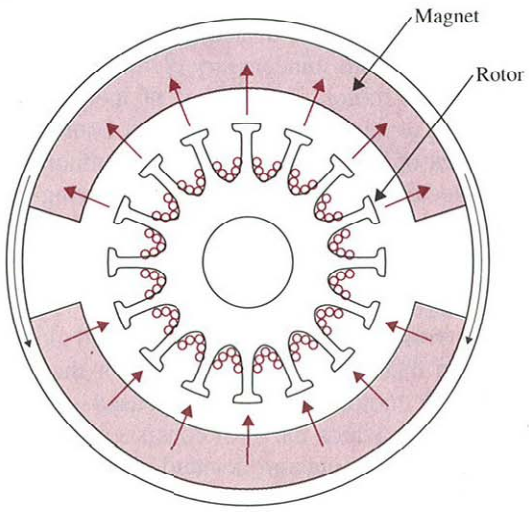

Figure 4-42 Cross-sectional view of a permanent-magnet iron-core dc motor.

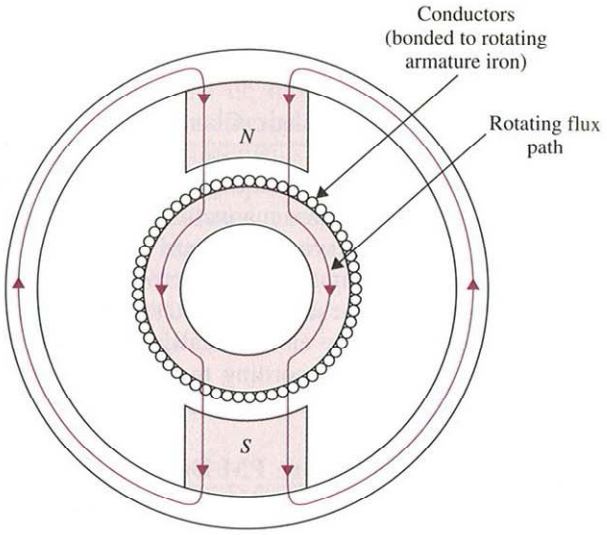

Figure 4-43 Cross-sectional view of a surface-wound permanent-magnet dc motor.

design, the armature has no "cogging" effect. Since the conductors are laid out in the air gap between the rotor and the permanent-magnet field, this type of motor has lower inductance than that of the iron-core structure.

Moving-Coil DC Motors

Moving-coil motors are designed to have very low moments of inertia and very low armature inductance. This is achieved by placing the armature conductors in the air gap between a stationary flux return path and the permanent-magnet structure, as shown in Fig. 4-44. In this case, the conductor structure is supported by nonmagnetic material—usually epoxy resins or fiber glass—to form a hollow cylinder. One end of the cylinder forms a hub, which is attached to the motor shaft. A cross-sectional view of such a motor is shown in Fig. 4-45. Since all unnecessary elements have been removed from the armature of the moving-coil motor, its moment of inertia is very low. Since the conductors in the moving-coil armature are not in direct contact with iron, the motor inductance is very low; values of less than 100 μH are common in this type of motor. The low-inertia and low-inductance properties make the moving-coil motor one of the best actuator choices for high-performance control systems.

Brushless DC Motors

Brushless dc motors differ from the previously mentioned dc motors in that they employ electrical (rather than mechanical) commutation of the armature current. The configuration of the brushless dc motor most commonly used—especially for incremental-motion applications—is one in which the rotor consists of magnets and "back iron" support, and whose commutated windings are located external to the rotating parts, as shown in Fig. 4-46. Compared to the conventional dc motors, such as the one shown

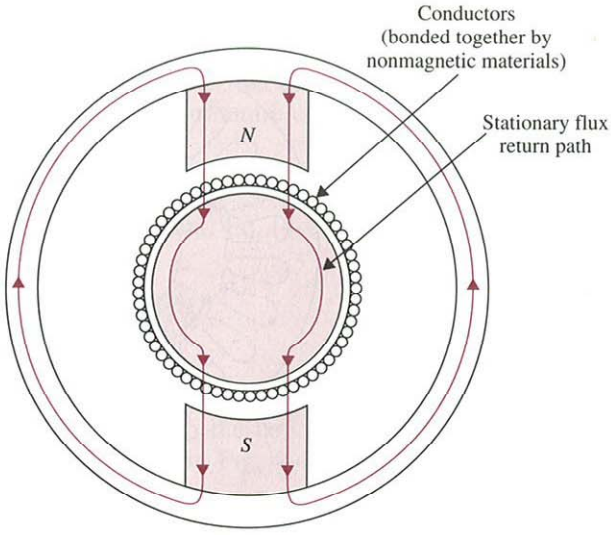

Figure 4-44 Cross-sectional view of a moving-coil permanent-magnet dc motor.

in Fig. 4-42, it is an "inside-out" configuration. Depending on the specific application, brushless dc motors can be used when a low moment of inertia is called for, such as the spindle drive in high-performance disk drives used in computers.

4-6-3 Mathematical Modeling of PM DC Motors

Since dc motors are used extensively in control systems, for analytical purposes, it is necessary to establish mathematical models for dc motors for control applications. We use the equivalent circuit diagram in Fig. 4-47 to represent a PM dc motor. The armature

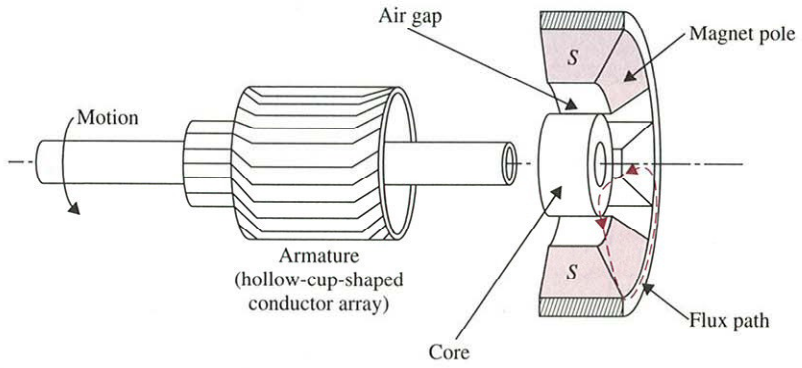

Figure 4-45 Cross-sectional side view of a moving-coil dc motor.

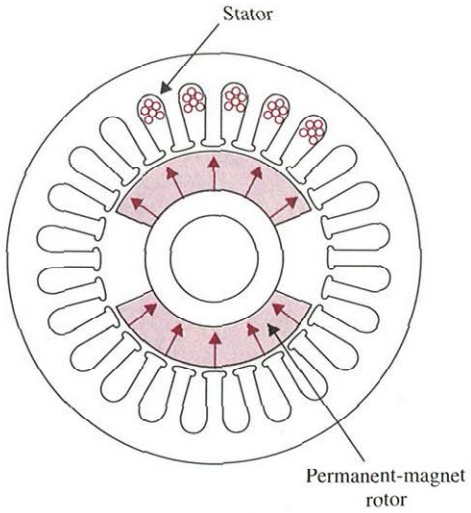

Figure 4-46 Cross-sectional view of a permanent-magnet brushless dc motor.

is modeled as a circuit with resistance R_a connected in series with an inductance L_a, and a voltage source e_b representing the back emf in the armature when the rotor rotates. The motor variables and parameters are defined as follows:

- $i_a(t)$ = armature current
- R_a = armature resistance
- $e_b(t)$ = back emf
- $T_L(t)$ = load torque
- $T_m(t)$ = motor torque
- $\theta_m(t)$ = rotor displacement
- K_i = torque constant
- L_a = armature inductance
- $e_a(t)$ = applied voltage
- K_b = back-emf constant
- ϕ = magnetic flux in the air gap
- $\omega_m(t)$ = rotor angular velocity
- J_m = rotor inertia
- B_m = viscous-friction coefficient

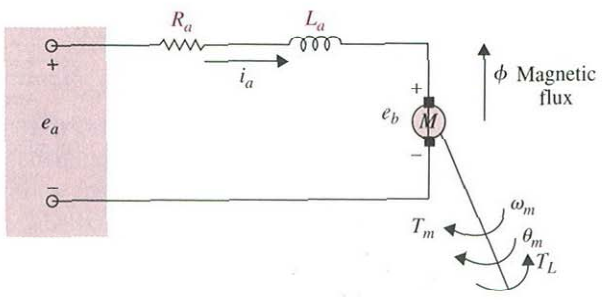

Figure 4-47 Model of a separately excited dc motor.

With reference to the circuit diagram of Fig. 4-47, the control of the dc motor is applied at the armature terminals in the form of the applied voltage $e_a(t)$. For linear analysis, we assume that the torque developed by the motor is proportional to the air-gap flux and the armature current. Thus

$$T_m(t) = K_m(t)\phi i_a(t) \tag{4-103}$$

Since ϕ is constant, Eq. (4-103) is written

$$T_m(t) = K_i i_a(t) \tag{4-104}$$

where K_i is the **torque constant** in N-m/A, lb-ft/A, or oz-in./A.

Starting with the control input voltage $e_a(t)$, the cause-and-effect equations for the motor circuit in Fig. 4-47 are

$$\frac{di_a(t)}{dt} = \frac{1}{L_a} e_a(t) - \frac{R_a}{L_a} i_a(t) - \frac{1}{L_a} e_b(t) \tag{4-105}$$

$$T_m(t) = K_i i_a(t) \tag{4-106}$$

$$e_b(t) = K_b \frac{d\theta_m(t)}{dt} = K_b \omega_m(t) \tag{4-107}$$

$$\frac{d^2\theta_m(t)}{dt^2} = \frac{1}{J_m} T_m(t) - \frac{1}{J_m} T_L(t) - \frac{B_m}{J_m} \frac{d\theta_m(t)}{dt} \tag{4-108}$$

where $T_L(t)$ represents a load frictional torque such as Coulomb friction.

Equations (4-105) through (4-108) consider that $e_a(t)$ is the cause of all causes; Eq. (4-105) considers that $di_a(t)/dt$ is the immediate effect due to the applied voltage $e_a(t)$, then in Eq. (4-106), $i_a(t)$ causes the torque $T_m(t)$, Eq. (4-107) defines the back emf, and finally, in Eq. (4-108), the torque $T_m(t)$ causes the angular velocity $\omega_m(t)$ and displacement $\theta_m(t)$.

The state variables of the system can be defined as $i_a(t)$, $\omega_m(t)$, and $\theta_m(t)$. By direct substitution and eliminating all the nonstate variables from Eqs. (4-105) through (4-108), the state equations of the dc-motor system are written in vector-matrix form:

$$\begin{bmatrix} \dfrac{di_a(t)}{dt} \\ \dfrac{d\omega_m(t)}{dt} \\ \dfrac{d\theta_m(t)}{dt} \end{bmatrix} = \begin{bmatrix} -\dfrac{R_a}{L_a} & -\dfrac{K_b}{L_a} & 0 \\ \dfrac{K_i}{J_m} & -\dfrac{B_m}{J_m} & 0 \\ 0 & 1 & 0 \end{bmatrix} \begin{bmatrix} \dfrac{1}{L_a} \\ 0 \\ 0 \end{bmatrix} e_a(t) - \begin{bmatrix} 0 \\ \dfrac{1}{J_m} \\ 0 \end{bmatrix} T_L(t) \tag{4-109}$$

Notice that in this case, $T_L(t)$ is treated as a second input in the state equations.

The state diagram of the system is drawn as shown in Fig. 4-48, using Eq. (4-109). The transfer function between the motor displacement and the input voltage is obtained from the state diagram as

$$\frac{\Theta_m(s)}{E_a(s)} = \frac{K_i}{L_a J_m s^3 + (R_a J_m + B_m L_a)s^2 + (K_b K_i + R_a B_m)s} \tag{4-110}$$

where $T_L(t)$ has been set to zero.

Figure 4-49 shows a block-diagram representation of the dc-motor system. The advantage of using the block diagram is that it gives a clear picture of the transfer-function relation between each block of the system. Since an s can be factored out from the denominator of Eq. (4-110), *the significance of the transfer function $\Theta_m(s)/E_a(s)$ is that the dc motor is essentially an integrating device between these two variables.* This is expected, since if $e_a(t)$ is a constant input, the output motor displacement will behave as the output of an integrator; that is, it will increase linearly with time.

▲ Dc motor is essentially an integrating device.

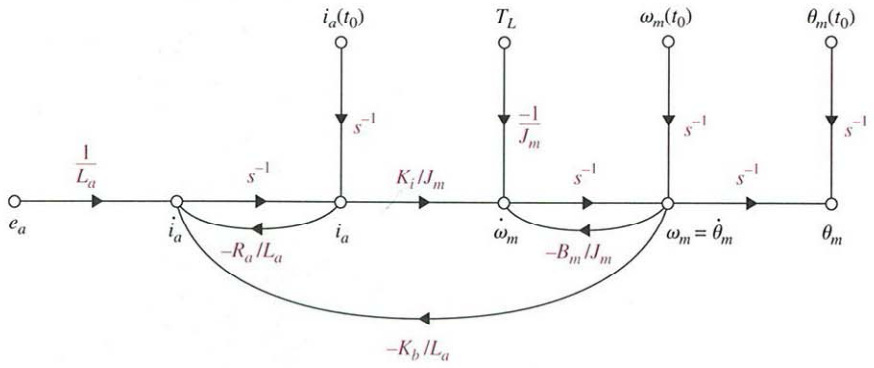

Figure 4-48 State diagram of a dc motor.

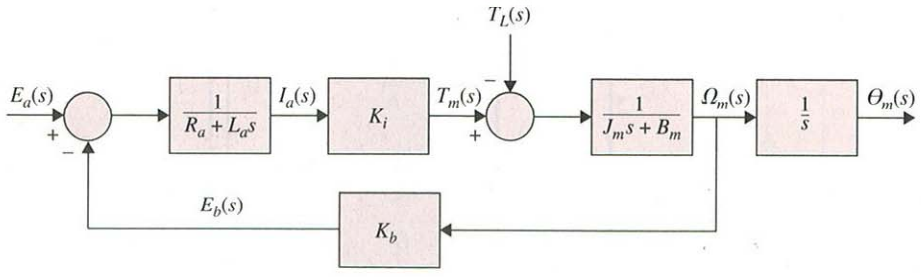

Figure 4-49 Black diagram of a dc motor system.

Although a dc motor by itself is basically an open-loop system, the state diagram of Fig. 4-48 and the block diagram of Fig. 4-49 show that the motor has a "built-in" feedback loop caused by the back emf. Physically, the back emf represents the feedback of a signal that is proportional to the negative of the speed of the motor. As seen from Eq. (4-110), the back-emf constant K_b represents an added term to the resistance R_a and the viscous-friction coefficient B_m. Therefore, *the back-emf is equivalent to an "electric friction," which tends to improve the stability of the motor, and in general, the stability of the system.*

▲ Back emf generally improves system stability.

Relation between K_i and K_b

Although functionally the torque constant K_i and back-emf constant K_b are two separate parameters, for a given motor, their values are closely related. To show the relationship, we write the mechanical power developed in the armature as

$$P = e_b(t)i_a(t) \tag{4-111}$$

The mechanical power is also expressed as

$$P = T_m(t)\omega_m(t) \tag{4-112}$$

where, in SI units, $T_m(t)$ is in N-m and $\omega_m(t)$ is in rad/sec. Now substituting Eqs. (4-106) and (4-107) in Eq. (4-111), we get

$$P = T_m(t)\omega_m(t) = K_b\omega_m(t)\frac{T_m(t)}{K_i} \tag{4-113}$$

from which we get

$$K_b \text{ (V/rad/sec)} = K_i \text{ (N-m/A)} \tag{4-114}$$

Thus we see that in the SI unit system, the values of K_b and K_i are identical if K_b is represented in V/rad/sec and K_i is in N-m/A.

In the British unit system, we convert Eq. (4-111) into horsepower (hp); that is,

$$P = \frac{e_b(t)i_a(t)}{746} \quad \text{hp} \tag{4-115}$$

In terms of torque and angular velocity, P is

$$P = \frac{T_m(t)\omega_m(t)}{550} \quad \text{hp} \tag{4-116}$$

where $T_m(t)$ is in ft-lb and $\omega_m(t)$ is in rad/sec. Using Eq. (4-106) and (4-107) and equating the last two equations, we get

$$\frac{K_b\omega_m(t)T_m(t)}{746K_i} = \frac{T_m(t)\omega_m(t)}{550} \tag{4-117}$$

Thus

$$K_b = \frac{746}{550}K_i = 1.356K_i \tag{4-118}$$

where K_b is in V/rad/sec and K_i is in ft-lb/A.

4-6-4 Torque–Speed Curves of a DC Motor

The torque–speed curves of a dc motor describe the static-torque-producing capability of the motor with respect to the applied voltage and motor speed. With reference to Fig. 4-50, in the steady state, the effect of the inductance is zero, and the torque equation of the motor is

$$T_m = K_iI_a = \frac{K_i(E_a - K_b\Omega_m)}{R_a} \tag{4-119}$$

where T_m, I_a, E_a, and Ω_m represent the steady-state values of the motor torque, current, applied voltage, and speed, respectively.

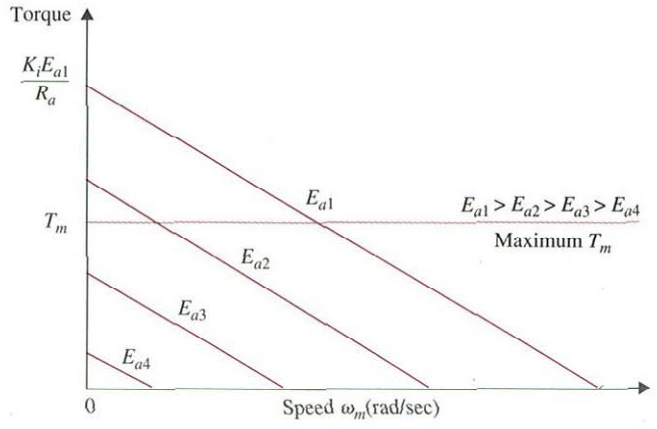

Figure 4-50 Typical torque–speed curves of a dc motor.

For a given applied voltage E_a, Eq. (4-119) describes the straight-line relation of the torque–speed characteristics of the dc motor. In reality, the motor may be subject to two types of saturation or limitations. One limitation is that as the armature current increases from the increase in E_a, the magnetic circuit will saturate, so that the motor torque cannot exceed a certain maximum value. The second limitation is due to the maximum current that the motor can handle due to the heat-dissipation rating of the motor.

Figure 4-50 shows a typical set of torque–speed curves for various applied voltages. The slope of these curves is determined from Eq. (4-119) and is expressed as

$$k = \frac{dT_m}{d\Omega_m} = -\frac{K_i K_b}{R_a} \tag{4-120}$$

The limit on the torque due to magnetic saturation is shown by the dashed line in the figure. In practice, the torque–speed curves of a dc motor can be determined experimentally by a dynamometer.

4-6-5 Torque–Speed Curves of an Amplifier/DC-Motor System

Since the dc motor is always driven by a power amplifier that acts as a source of energy, it is more practical to present the torque–speed curves of the amplifier–motor combination, especially if the amplifier gain is subject to saturation. Figure 4-51 shows the equivalent block diagram of an amplifier–motor system. The amplifier has a gain of K_1. The saturation level of the output voltage of the amplifier is E_L. Current feedback with gain K_L is also introduced for stabilization of the system. The steady-state torque equation of the system is written from Fig. 4-51 by treating E_{in} and Ω_m as inputs, and T_m as the output. When the amplifier is not saturated, the motor torque is

$$T_m = \frac{K_i(K_1 E_{\text{in}} - K_b \Omega_m)}{R_a + K_1 K_2} \tag{4-121}$$

Without amplifier saturation, the torque–speed curves described by Eq. (4-121) are again a family of straight lines, as illustrated in Fig. 4-50. The slope of the torque–speed curves is

$$k = \frac{dT_m}{d\Omega_m} = -\frac{K_1 K_b}{R_a + K_1 K_2} \tag{4-122}$$

Comparing Eq. (4-122) with Eq. (4-120), we see that the effect of the current feedback of the amplifier is that the gain K_2 reduces the slope of the torque–speed curves of the motor.

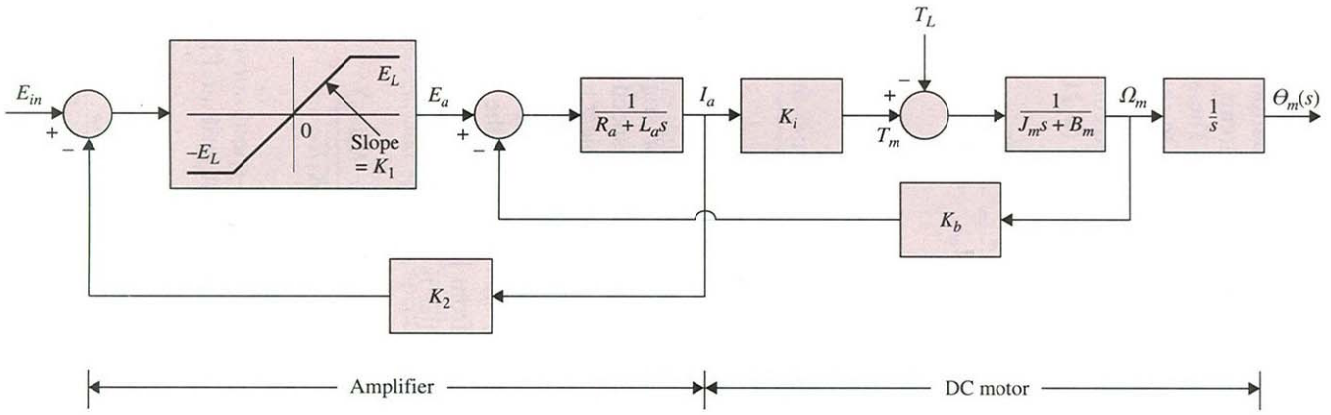

Figure 4-51 Equivalent block diagram of an amplifier/dc-motor system.

When the amplifier is subject to saturation, $|E_a| \leq E_L$. When $|E_a| = E_L$, the torque equation in the steady state is

$$T_m = \frac{K_i}{R_a}(E_L - K_b\Omega_m) \tag{4-123}$$

This gives the maximum blocked-rotor ($\Omega_m = 0$) torque as $T_m = K_iE_L/R_a$. The slope of the torque–speed curve under amplifier saturation is $-K_iK_b/R_a$. Figure 4-52 shows the torque–speed curves of the amplifier–motor combination when the amplifier is subject to saturation.

4-7 Linearization of Nonlinear Systems

From the discussions given in the preceding sections, we should realize that most components and actuators found in physical systems have nonlinear characteristics. In practice, we may find that some devices have moderate nonlinear characteristics, or the nonlinear properties would occur if they are driven into certain operating regions. For these devices, modeling by linear system models may give quite accurate analytical results over a relatively wide range of operating conditions. However, there are numerous physical devices that possess strong nonlinear characteristics. For these devices, strictly, a linearized model is valid only for a limited range of operation, and often only at the

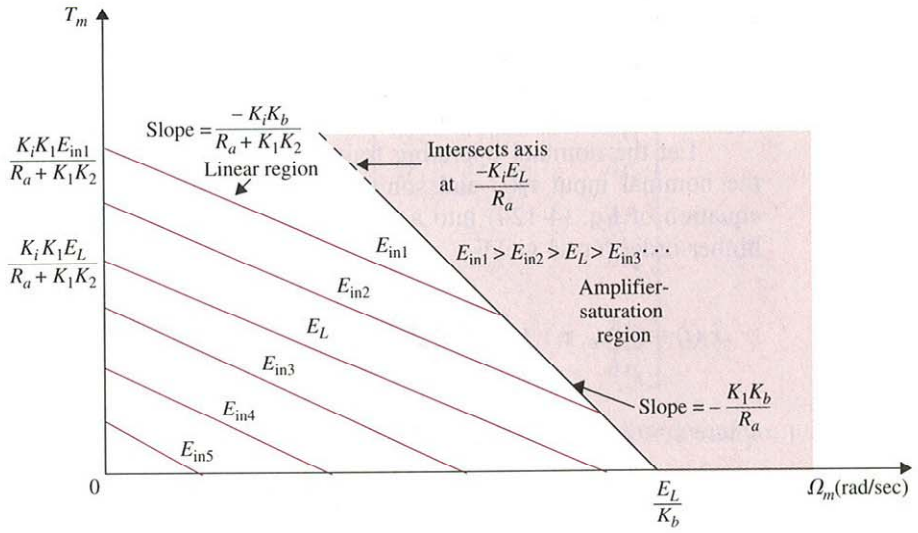

Figure 4-52 Torque–speed curve of amplifier/dc-motor system with amplifier saturation and current feedback.